

Two conserved arginine residues from the SK3 potassium channel outer vestibule control selectivity of recognition by scorpion toxins.

Jing Feng, Youtian Hu, Hong Yi, Shijin Yin, Song Han, Jun Hu, Zongyun Chen, Weishan Yang, Zhijian Cao, Michel de Waard, et al.

▶ **To cite this version:**

Jing Feng, Youtian Hu, Hong Yi, Shijin Yin, Song Han, et al.. Two conserved arginine residues from the SK3 potassium channel outer vestibule control selectivity of recognition by scorpion toxins.: Key Residues of SK3 Channel for Selective Toxin Recognition. Journal of Biological Chemistry, 2013, 288 (18), pp.12544-53. 10.1074/jbc.M112.433888 . inserm-00842942

HAL Id: inserm-00842942

https://inserm.hal.science/inserm-00842942

Submitted on 14 Mar 2014

HAL is a multi-disciplinary open access archive for the deposit and dissemination of scientific research documents, whether they are published or not. The documents may come from teaching and research institutions in France or abroad, or from public or private research centers.

L'archive ouverte pluridisciplinaire **HAL**, est destinée au dépôt et à la diffusion de documents scientifiques de niveau recherche, publiés ou non, émanant des établissements d'enseignement et de recherche français ou étrangers, des laboratoires publics ou privés.

Title

Two Arginine Residues from the SK3 Channel Outer Vestibule Controls Selectivity of Recognition by Scorpion Toxins

Jing Feng[1†], Youtian Hu[1†], Hong Yi[1†], Shijin Yin[1], Song Han[1], Jun Hu[1], Zongyun Chen[1], Weishan Yang[1], Zhijian Cao[1], Michel De Waard[2,3], Jean-Marc Sabatier[4], Wenxin Li[1] and Yingliang Wu[1*]

[1]State Key Laboratory of Virology, College of Life Sciences, Wuhan University, Wuhan 430072, P.R. China.

[2]Inserm U836, Grenoble Neuroscience Institute, Laboratory of Excellence 'Ion Channels Science and Therapeutics', Université Joseph Fourier, Bâtiment Edmond Safra, 38042 Grenoble Cedex 09, France.

[3]Smartox Biotechnology, Bâtiment Biopolis, 5 avenue du Grand Sablon, 38700 La Tronche, France.

[4]Inserm UMR1097, Aix-Marseille Université, Parc Scientifique de Luminy, 13288 Marseille, France.

Running title

Key Residues of SK3 Channel for Selective Toxin Recognition

*Correspondence to Professor Yingliang Wu

Address: State Key Laboratory of Virology, College of Life Sciences, Wuhan University, Luojia Hill, Wuhan 430072, P.R. China.
Tel.: +086-27-6875 2831 - Fax: +086-27-6875 6746 - E-mail: ylwu@whu.edu.cn

Number of text pages: 23

Number of tables: 0

Number of figures: 6

Number of references: 38

Number of words in the *Abstract*: 251

Number of words in *Introduction*: 947

Number of words in *Discussion*: 962

Nonstandard abbreviations: BK, large conductance calcium-activated potassium channel; BmP05, *Buthus martensii karsch* P05 toxin; ChTX, Charybdotoxin; hERG, human *ether-à-go-go*-related gene; KCa, Ca^{2+}-activated K^+ channels; Kir, inwardly rectifying two-transmembrane K^+ channels; K2P, two-pore K^+ channels; MD, molecular dynamics; SK3 channel, small conductance calcium-activated potassium channel type 3; K_v channel, voltage-gated potassium channel; ScyTx, scyllatoxin.

ABSTRACT

Potassium channel functions are often deciphered by the use of selective and potent scorpion toxins. Among these toxins, only a limited subset is capable to selectively block small conductance Ca^{2+}-activated K^+ (SK) channels. The structural bases of this selective SK channel recognition still remain unclear. In this work, we demonstrate the key role of the electric charges of two conserved arginine residues (R^{485} and R^{489}) from the SK3 channel outer vestibule in the selective recognition by SK3-blocking BmP05 toxin. Indeed, individually substituting these residues by histidyl or lysyl (maintaining partially or fully the positive electric charge), while decreasing the affinity of BmP05, still preserves its toxin-sensitivity profile (as evidenced by the lack of recognition by the voltage-gated potassium channel (K_v)-blocking charybdotoxin (ChTX)). In contrast, when R^{485} or R^{489} residue of SK3 channel is mutated towards an acidic (E) or alcoholic (S) amino acid residue, the channel loses its sensitivity to BmP05 and becomes susceptible to a 'new' blocking activity by ChTX. Besides these basic SK3 channel residues important for sensitivity, two acidic D^{492} and D^{518} residues, also located in the SK3 channel outer vestibule, were identified as being critical for toxin affinity. Further, molecular modeling data indicate the existence of a compact SK3 channel turret conformation where the basic rings of R^{485} and R^{489} residues are stabilized by strong ionic interactions with the acidic D^{492} and D^{518} residues. In conclusion, the unique properties of R^{485} and R^{489} residues (spatial orientations and molecular interactions) of SK3 channel account for its toxin-sensitivity profile.

INTRODUCTION

With about one hundred members, the potassium channel family serves a variety of physiological functions and is involved in various channelopathies (Ashcroft, 2006). Based on their activation mode and number of transmembrane segments, these channels can be classified according to four main structural types: (i) inwardly rectifying two-transmembrane K^+ channels (Kir), (ii) two-pore K^+ channels with four transmembrane segments (K2P), (iii) Ca^{2+}-activated K^+ channels with six or seven transmembrane segments (KCa), and (iv) voltage-gated K_v channels with six transmembrane segments. Scorpion toxins are widely used to distinguish between these potassium channel types (Gross and MacKinnon, 1996; Lu et al., 2001; MacKinnon et al., 1998). Crystal structures of various potassium channels have recently been published markedly increasing our knowledge of ion channel pores, selectivity filters, and gates (Doyle et al., 1998; Long et al., 2005; Tao et al., 2009). In two crystal structures of eukaryotic K_v1.2 and Kir2.2 channels, significant structural differences can be observed in the extracellular pore entryway, including turrets and filter regions, which are responsible for channel inactivation, toxin recognition, and interactions between channel subunits (Fig. S1). In contrast to the K_v1.2 extracellular pore entryway structure, the large turret and unusual TIGYGLR sequence in the filter region of Kir2.2 are responsible for its relative insensitivity to K^+ channel toxins (Long et al., 2005; Tao et al., 2009). In addition to these structural differences in the extracellular pore entryways between eukaryotic K_v1.2 and Kir2.2 channels, other specific structural differences have been identified by using scorpion toxins as molecular probes. In human *ether-à-go-go*-related gene (hERG) channel (Fig. S1), also referred to as K_v11.1, unusually long turrets likely form a decentralized ‘petunia’ shape which could be probed by scorpion toxin BeKm-1 (Yi et al., 2007). Alternative models without a petunia shape are also proposed for the hERG channel turret (Subbotina et al., 2010; Tseng et al., 2007). The conformation of the large conductance calcium-activated potassium (BK) channel turret varies from an open-state one, for ChTX recognition, to an “helmet” one,

for ChTX insensitivity, when the channel turret associates to the auxiliary β4 subunit (Gan et al., 2008) (Fig. S1). Overall, progress in characterizing extracellular pore entryways has demonstrated their significant structural and functional diversities. However, because of the present difficulty to solve crystal structures of additional eukaryotic potassium channels, further characterization of extracellular pore entryways of other potassium channels with unique functions remains a challenge.

Small conductance calcium-activated (SK) channels are predominantly present in the nervous system (Berkefeld et al., 2010; Stocker, 2004). They are involved in synaptic plasticity, fast glutamatergic synaptic potentials, and hippocampal learning (Faber et al., 2005; Hammond et al., 2006; Stackman et al., 2002). SK channels are efficiently blocked by several scorpion toxins such as BmP05, scyllatoxin (ScyTx), and P05, but are insensitive towards many others (Han et al., 2010; Rodriguez de la Vega and Possani, 2004). Very few reports investigate the structural features that underlie the specific recognition of SK channels by a restricted set of scorpion toxins. According to these studies, SK channel blockade would occur according to an 'intermediate' mode of interaction (Rodriguez de la Vega et al., 2003) involving mainly the toxin alpha helical structure rather than its β-sheet structure (Cui et al., 2002; Regaya et al., 2004; Andreotti et al., 2005). Two arginyl residues, found in a RRCQ motif present in both P05 and apamin, were critical for P05 interaction with its target, as described for apamin (Sabatier et al., 1993). In contrast, the β-sheet structure appears rather important for a 'pore-blocking' mode as far as K_v channel block is concerned (Rodriguez de la Vega et al., 2003; Yu et al., 2005; Lange et al., 2006). This distinctive mode of operation between SK channel-blocking and K_v channel-blocking toxins may be reconsidered taking into account the current state of knowledge on toxin interaction and computer-based simulation of toxin docking. Indeed, earlier studies were conducted based on less efficient docking simulations and evidence is now rising that the mode of toxin interaction with potassium channels may be switchable. In addition, channel turrets seem to play an important

role in toxin docking. SK channel turret acidic residues were found to be involved in toxin binding in the 'intermediate' mode (Wittekindt et al., 2004; Andreotti et al., 2005). Evidence has been provided that SK channel block by an MTX-HsTx1 chimera is dependent on ionic strength, suggesting that SK channel recognition by scorpion toxins involves some electrostatic charges (Shakkotai et al., 2001; Castle et al., 2003). Acidic amino acid residues of toxins were found to affect the interaction modes further strengthening the importance of electrostatic interactions between toxins and channels (Han et al., 2010). Herein, we explored the importance of electrostatic repulsion for the interaction of the alpha helical structure of BmP05 with SK3 channel. Introducing positively charged residues within the alpha helical structure of BmP05 decreases toxin affinity. After identification of key positively-charged residues of SK3 channel turret (two conserved arginine residues at turret positions 485 and 489) and relevant mutations, we were able to render the SK3 channel sensitive to ChTx block by its β-sheet surface owing to its strong content in basic amino acid residues in spite of the fact that ChTx is pharmacologically unrelated to BmP05. Our data demonstrate that the mode of toxin / channel interaction can be altered by selective point mutations of the channel with the aid of appropriate computer-aided molecular simulations. We also evidenced that the toxin-sensitivity profile of SK3 channels is controlled by two conserved turret arginine residues that produce differential repulsive electrostatic forces with basic residues of scorpion toxins. These results further boost our understanding of the structural and functional diversity of potassium channel extracellular pore entryways and unlocks the pharmacological potential of toxins.

MATERIALS AND METHODS

Materials. Non specified chemicals were obtained from Sigma.

Toxins, toxin analogs and potassium channels. BmP05 and its mutants, ChTX, and ADWX-1 were prepared according to a procedure described previously (Han et al., 2008). pEGFP-N1 plasmid containing the full-length human SK3 cDNA sequence was kindly provided by Prof. Stephan Grissmer (University of Ulm, Ulm, Germany). Point mutations in SK3 channel were generated using the Quikchange mutagenesis kit (Stratagene). All cDNA mutants were confirmed by DNA sequencing (Invitrogen).

Cell culture. Human embryonic kidney (HEK293) cells were cultured in Dulbecco's modified Eagle's medium (Invitrogen) supplemented with 10% fetal bovine serum and 1% penicillin/streptomycin in a humidified 5% CO_2 incubator at 37°C. Cells were transfected using FuGene Transfection Reagent (Roche Diagnostics, Switzerland) following the manufacturer's instructions and used for electrophysiology 24–48 h after transfection.

Electrophysiology and data analyses. Electrophysiological experiments were performed at a temperature of 22–25°C using the patch-clamp whole-cell recording mode. For channel recording, ionic compositions are as follows. The bath medium contained (in mM): sodium aspartate 130, potassium aspartate 30, $CaCl_2$ 2, $MgCl_2$ 1, and HEPES 10 (pH 7.4 with NaOH). The pipette solution contained (in mM): potassium aspartate 145, $CaCl_2$ 8.7, $MgCl_2$ 2, EGTA 10, and HEPES 10 (pH 7.2 with KOH). Intra-pipette free Ca^{2+} concentration is estimated to be 1 μM. Membrane potentials were clamped to -120 mV for 50 ms followed by a 400 ms voltage ramp from -120 to +60 mV and were kept for 5 s between ramps at -40 mV using a HEKA EPC10 amplifier with Patchmaster (HEKA Elektronik, Germany) as data acquisition software. Data analyses were performed with IGOR software (WaveMetrics, Lake Oswego, OR, USA). The IC_{50} values were obtained by fitting a modified Hill equation to the data as shown in Equation 1: $I_{toxin}/I_{control}=1/ (1+ ([\text{toxin peptide}]/IC_{50}))$ where I is the normalized

current at -120 mV without ($I_{control}$) or with at least five different toxin peptide concentrations (I_{toxin}). Results are shown as mean ± s.e.m. of at least three experiments.

Atomic coordinates and molecular docking. With the exception of the turret, the spatial structure of the SK3 pore region was modeled using the crystallographic structure of the KcsA channel (PDB code: 1BL8) as a template using the SWISS-MODEL server (Guex and Peitsch, 1997). The SK3 turret was built using the segment-assembly homology modeling method, as described previously (Gan et al., 2008; Yi et al., 2007). An additional unrestrained molecular dynamics (MD) simulation was performed on the model to get an equilibrated SK3 channel structure. The 3D structure of BmP05 was modeled using the atomic coordinates of the 90% identical ScyTx (PDB code: 1SCY). BmP05 was docked onto the equilibrated SK3 channel structure using the ZDOCK program (Chen et al., 2003). Clustering analysis and experimental data-based screening were used to identify possible hits from the resulting complexes. These hits were then subjected to further MD simulation to evaluate their structural stability.

Molecular dynamics simulations. MD simulations were performed using the AMBER 11 program on a 128-CPU Dawning TC5000 cluster (Beijing, P.R. China). The ff99 force-field (Parm 99) (Wang, 1999) was applied throughout all the simulation steps. Both the SK3 channel and BmP05-SK3 complex structures were subjected to unrestrained simulations in explicit solvent systems. The SK3 channel and BmP05-SK3 complexes were first embedded in periodic boxes of 71.755 × 79.440 × 79.589 Å and 74.141 × 80.972 × 81.867 Å, respectively. A 5 ns pre-equilibration, followed by a 10 ns unrestrained simulation, were performed on SK3 channel and channel-toxin complex using the SANDER module in the AMBER11 program to get enough stable conformations. The pre-equilibration steps were performed by gradually reducing the force constant from 5.0 (kcal/mol)/$Å^2$ for restraining all the heavy atoms to 0.02 (kcal/mol)/$Å^2$ for backbone heavy atoms only. The temperature was set at 300K with a cut-off distance of 10 Å.

RESULTS

The SK3 channel is selectively inhibited by scorpion toxins exhibiting no more than three basic amino acid residues in their channel binding interfaces. As shown, SK3 channels are almost insensitive to 100 nM of the K_v channel- and BK channel-acting ChTX (Figs. 1a and S2a) or K_v-channel-acting ADWX-1 (Han et al., 2008) (Fig. 1b). In contrast, 100 nM BmP05 inhibits ca. 80% of the SK3 channel current (Fig. 1c). The corresponding IC_{50} value of BmP05-induced current block is 3.8 nM (Fig. 3d). Structurally, there are four basic amino acid residues at close vicinity of the pore-blocking basic K^{27} residue of ChTX or K^{26} residue of ADWX-1 (Figs. 1e, f). In contrast, the channel binding interface of BmP05 or ScyTx presents only three (Fig. 1g) or two basic residues (Fig. 1h) (Pease and Wemmer, 1988; Wu et al., 2002). These structural differences in channel binding interfaces suggest that the SK3 channel may be selectively recognized by scorpion toxins possessing three (or less) basic residues in these critical positions.

To further characterize the BmP05 binding interface, we tested the effect of adding extra basic residue(s) on its ability to recognize the SK3 channel (Fig. 2a). Increasing the number of basic residues by one (at BmP05 position 14 or 15) or two arginyl residues (at BmP05 positions 4 and 14, or 4 and 15), strongly reduced its inhibitory potency at 100 nM concentration on SK3 currents (Figs. 2b-e). This decreased potency was stronger when two extra arginyl residues were incorporated in BmP05 binding interface (BmP05-N4R/S14R and BmP05-N4R/L15R) instead of a single one (BmP05-S14R and BmP05-L15R) (see Figs. 2d, e *versus* 2b, c). From the data, it appears that an efficient block of the SK3 channel by BmP05 occurs when three basic residues are located in the channel binding interface of the toxin.

Substitution of SK3 channel R^{485} or R^{489} basic residue by other basic residues impairs BmP05 affinity but maintains the differential BmP05/ChTX sensitivity for the SK3

channel. The sensitivity of BmP05 to the presence of extra basic amino acid residues in the toxin binding interface strongly suggests the important role of electrostatic repulsion forces between BmP05 binding interface and SK3 channel binding site. These electrostatic repulsion forces might occur with R^{485} and R^{489} residues, two highly conserved basic residues that are located in the outer vestibules of all SK channel subtypes (Fig. S1). These electrostatic repulsion forces, if actually existing, can be diminished by replacing the wild-type R^{485} or R^{489} residue of the SK3 channel by less basic lysyl (SK3-R485K and SK3-R489K) or histidyl (SK3-R485H and SK3-R489H) residues. The resulting mutated channels were still insensitive to 100 nM ChTX application (Figs. 3a, b, e, f), but maintained their sensitivity to 100 nM BmP05 (Figs. 3c, d, g, h), albeit at reduced levels. The degree of reduction in BmP05 effect was assessed by dose-response analyses indicating affinity reductions of the mutated channels for BmP05 by 88- (SK3-R485H), 101- (SK3-R489H), 38- (SK3-R485K), 51-fold (SK3-R489K) (Figs. 3i, j). The reduction in affinity is higher for the R to H mutations, as expected from the least basic nature of histidyl residue. The basic nature of the amino acid residues at SK3 positions 485 and 489 (e.g. R, K or H) is key to maintain the BmP05/ChTX selectivity towards the SK3 channel, while the presence of arginyl residues at these positions is mandatory to maintain high BmP05 affinity.

Replacement of R^{485} and R^{489} residues of SK3 channel by acidic or polar residues alters its relative sensitivity to BmP05/ChTX. An additional step in weakening the electrostatic repulsion forces at the toxin/channel binding interface is to substitute the SK3 channel dyad of arginyl by acidic or polar amino acid residues. This was achieved by replacing R^{485} or R^{489} by a glutamic acid (acidic) or serine (polar) residue in SK3 channel. In agreement with the importance of R^{485} and R^{489} in the high affinity of BmP05 for SK3 channel, 100 nM BmP05 produced much less inhibition of SK3-R485E (Fig. 4a), SK3-R489E (Fig. 4b), SK3-R485S (Fig. 4e), and SK3-R489S (Fig. 4f) mutant channels, compared to the inhibition observed for

wild-type SK3 channel (Fig. 1c, d). The electrically neutral serine residue is less prone to alter the electrostatic balance at toxin/channel binding interface than the glutamic acid residue. This is coherent with the better current blocks of BmP05 on SK3-R485S and SK3-R489S mutant channels, as compared to the current blocks observed on SK3-R485E and SK3-R489E mutants. These data indicate that substitutions at positions 485 and 489 of SK3 channel are sufficient to make the channel almost insensitive to BmP05, further strengthening the idea that these SK3 channel positions are key to toxin recognition. Interestingly, the potassium currents carried by all tested mutant channels were significantly blocked by 100 nM ChTX (Figs. 4c, d, g, h). Dose-response analyses provide IC_{50} values of ChTX-induced current blocks of 381 nM (SK3-R485E), 110 nM (SK3-R489E), 84 nM (SK3-R485S), and 30 nM (SK3-R489S) (Figs. 4i, j). These data are remarkable in the sense that a toxin, ChTX, known to block only K_v and BK channel types, can gain a novel activity towards the SK3 channel if the later is appropriately mutated at position 485 or 489. Furthermore, it is worth mentioning that, in this case, the appropriate mutations of the SK3 channel allow the channel to invert its pharmacological toxin sensitivity recognition profile, from a BmP05-sensitive and ChTX-insensitive profile for wild-type SK3 channel to a BmP05-insensitive and ChTX-sensitive one for the appropriately mutated SK3 channel. Interestingly, these mutated SK3 channels acquire a pharmacological toxin sensitivity profile that resembles that of K_v channels, which are also BmP05-insensitive (Han et al., 2010) and ChTX-sensitive (Fig. S2a).

Influence of other amino acid residues from the outer vestibule on the relative SK3 channel sensitivity to BmP05/ChTX. Besides the dyad of arginyl residues (R^{485} and R^{489}), we also investigated the effects of mutating other residues from the outer vestibule of the SK3 channel on its toxin-sensitivity profile. Many mutated SK3 channels were found to be inactive (SK3-E488A, SK3-E488N, SK3-Y490A, SK3-H491A, SK3-D492A, SK3-D495A and SK3-D518A) and could not be investigated on this issue. However, five additional mutations

(SK3-D492N, SK3-Q493A, SK3-D495N, SK3-D518N and SK3-H522A) provided functional channels that could be characterized for their BmP05 and ChTX current blocks (Figs. 5a-e). Two channels (SK3-D492N and SK3-D518N) affected current block by 100 nM BmP05 (Figs. 5a, d, k), while three others (SK3-Q493A, SK3-D495N and SK3-H522A) maintained an efficient BmP05 block (Figs. 5b, c, e, k). Experimental IC_{50} values for the later channel mutants were 16 nM (SK3-Q493A), 17 nM (SK3-D495N), and 82 nM (SK3-H522A) (Fig. S2b). All SK3 channel mutants kept the toxin-sensitivity profile since none of the currents carried by these channels could be efficiently blocked by 100 nM ChTX (Figs. 5f-j, l). These data clearly highlight the particular contribution of the arginyl dyad of the SK3 channel outer vestibule in defining its selective recognition by toxins.

DISCUSSION

Extracellular pore entryways are structurally important elements of potassium channels. They are involved in several functions including channel inactivation, subunit interactions, and channel pharmacology. Due to the difficulties in solving potassium channel crystal structures (Long et al., 2005; Tao et al., 2009), potent scorpion toxins can be used to unravel potassium channel structure and function. Also, significant conformational rearrangements in the toxin / channel recognition surfaces have been investigated and/or evidenced by computational simulation techniques (Gan et al., 2008; Yi et al., 2007; Yin et al., 2008) and by solid-state NMR spectroscopy (Ader et al., 2009; Ader et al., 2008; Lange et al., 2006). Herein, we have investigated the SK3 channel structural determinants that are involved in the selective recognition by scorpion toxins by using BmP05 and ChTX as molecular probes. Our results point to the importance of a basic dyad, comprising the SK-conserved R^{485} and R^{489} residues of the channel turret, as a critical structural determinant in defining the efficacy whereby SK3 channel preferentially recognizes BmP05 over ChTX. Two questions deserve further attention. First, how does this dyad of SK3 residues impair the recognition of scorpion toxins such as ChTX? Second, how does the dyad influence the affinity/potency of SK3 channel-active toxins, such as BmP05, for SK3 channels?

In an attempt to solve these questions, we modeled the structures of both SK3 channel alone and SK3-BmP05 complex using molecular modeling techniques (Gan et al., 2008; Yi et al., 2007). As shown in Figs. 6a and 6b, the SK3 channel turret adopts a unique conformation, in which both R^{485} and R^{489} residues form salt bridges with aspartic acid residues from adjacent SK3 subunits (R^{485} with D^{492} residue, and R^{489} with both D^{492} and D^{518} residues). These internal electrostatic interactions between the four channel turrets contribute to the formation of a narrow gateway together with the large ring (four R^{485} residues) and small ring (four R^{489} residues) of basic residues, which is indicated by the structural superimposition of SK3 with $K_v1.2$ and Kir2.2 structures (Fig. S3). These two rings of basic amino acid residues

are conserved in the SK3-BmP05 complex structure (Fig. 6c). The unique structural properties (positions and interactions) of R^{485} and R^{489} residues may well account for the efficacy in governing scorpion toxin sensitivity for SK3 channel. As shown by the mutagenesis studies, SK3 channel dyad made of R^{485} and R^{489} residues is responsible for the toxin sensitivity of SK3 channels through differential electrostatic repulsion forces (Figs. 1 & 2). To minimize such forces, K^6 residue of BmP05 blocks the channel pore (Figs. 6c & d), similarly to K^{27} of ChTX or K^{26} of ADWX-1 (Gan et al., 2008; Han et al., 2008). The R^7 residue of BmP05 locates in between two R^{489} residues that form the small ring of basic residues, while toxin R^{13} hangs just above the two rings of R^{485} and R^{489} residues (Fig. 6c). Obviously, toxins with a greater number of basic amino acid residues in the channel-interacting surface are unable to recognize the SK3 channel owing to stronger electrostatic repulsion forces between toxin and basic rings of arginine residues (as evidenced in Figs. 1 and 2). The toxin recognition profile of SK3 channels (sensitive to BmP05 and insensitive to ChTX) is maintained by basic amino acid substitutions of the arginyl dyad (Fig. 3), but inverted by acidic or polar amino acid residue replacements (Fig. 4). At the structural level, these results can be interpreted by the maintenance or disappearance of basic rings depending on the nature of residue substitutions, i.e. preserved if the dyad is mutated towards basic amino acid residues, and lost if acidic or polar residues are selected instead. In that respect, it is interesting to note that the loss of one of the two basic rings 'derives' an SK3 channel towards a K_v-type channel by rendering the modified SK3 channel insensitive to BmP05 (Han et al., 2010) and sensitive to ChTX (Fig. S2a). Altogether, functional and modeling data point to an exquisite role of the two conserved R^{485} and R^{489} residues as being essential determinants of SK3 channel with regard to its recognition profile of toxins.

It is worth emphasizing that the two conserved R^{485} and R^{489} residues of the SK3 channel are also essential for the potency of SK3-blocking toxins by maintaining the unique narrow gateway conformation of the channel turrets (Figs. 6a & b), which are critical domains for

scorpion toxin interactions (Figs. 6e, f). The BmP05 affinity for the SK3 channel dropped significantly when those arginyl residues are replaced by less basic ones (Fig. 3). This may result in a looser conformation of the channel turrets as a consequence of weaker electrostatic interactions between the four SK3 channel subunits (Figs. 6a & b). The looser turret structure presumably impairs the interactions between BmP05 R^{7} and R^{13} residues with the critical residues from SK3 channel turrets (Figs. 6e, f). The D492N or D518N mutation, conferring BmP05 insensitivity to modified SK3 channels (Fig. 5), also disrupts some key electrostatic interactions between channel subunits, thereby conferring looser turret structures (Figs. 6a & b). These data strongly suggest that the potency of SK3-blocking scorpion toxins is dependent on the narrow gateway structure of SK3 outer vestibule, itself constrained by the electrostatic interactions of R^{485} and R^{489} with acidic residues.

In conclusion, this work describes the unique properties of two conserved SK3 channel R^{485} and R^{489} residues in controlling selective scorpion toxin recognition. Our findings likely contribute to a better understanding of the molecular mechanisms involved in the selective recognition of SK channels by scorpion toxins. Undoubtedly, it provides structural and mechanistic insights for the design of selective peptide inhibitors specific to each subtype of SK channel. Indeed, subtype-specific SK channel blockers would be useful to more effectively treat neurological disorders (Wulff and Zhorov, 2008).

ACKNOWLEDGMENTS

We greatly thank Prof. Stephan Grissmer (University of Ulm, Ulm, Germany) for assistance in electrophysiology.

AUTHORSHIP CONTRIBUTIONS

Participated in research design: Yi, Cao, Li and Wu

Conducted experiments: Feng, Hu, Yi, Yin and Hu

Contributed new reagents or analytic tools: Han, Chen and Yang

Performed data analysis: Feng, Hu, Yi, Yin, Hu, Li and Wu

Wrote or contributed to the writing of the manuscript: Wu, Sabatier and De Waard

REFERENCES

Ader C, Schneider R, Hornig S, Velisetty P, Vardanyan V, Giller K, Ohmert I, Becker S, Pongs O and Baldus M (2009) Coupling of activation and inactivation gate in a K^+-channel: potassium and ligand sensitivity. *EMBO J* **28**(18): 2825-2834.

Ader C, Schneider R, Hornig S, Velisetty P, Wilson EM, Lange A, Giller K, Ohmert I, Martin-Eauclaire MF, Trauner D, Becker S, Pongs O and Baldus M (2008) A structural link between inactivation and block of a K^+ channel. *Nat Struct Mol Biol* **15**(6): 605-612.

Andreotti N, di Luccio E, Sampieri F, De Waard M and Sabatier JM (2005) Molecular modeling and docking simulations of scorpion toxins and related analogs on human SKCa2 and SKCa3 channels. *Peptides* **26**(7): 1095-1108.

Ashcroft FM (2006) From molecule to malady. *Nature* **440**(7083): 440-447.

Berkefeld H, Fakler B and Schulte U (2010) Ca^{2+}-activated K^+ channels: from protein complexes to function. *Physiol Rev* **90**(4): 1437-1459.

Castle NA, London DO, Creech C, Fajloun Z, Stocker JW and Sabatier JM. Maurotoxin: a potent inhibitor of intermediate conductance Ca2+-activated potassium channels. *Mol Pharmacol* **63**(2): 409-418.

Chen R, Li L and Weng Z (2003) ZDOCK: an initial-stage protein-docking algorithm. *Proteins* **52**(1): 80-87.

Cui M, Shen J, Briggs JM, Fu W, Wu J, Zhang Y, Luo X, Shi Z, Jiang H and Chen K (2002) Brownian dynamics simulations of the recognition of the scorpion toxin P05 with the small-conductance calcium-activated potassium channels. *J Mol Biol* **318**(2): 417-428.

Doyle DA, Morais Cabral J, Pfuetzner RA, Kuo A, Gulbis JM, Cohen SL, Chait BT and MacKinnon R (1998) The structure of the potassium channel: molecular basis of K^+ conduction and selectivity. *Science* **280**(5360): 69-77.

Faber ES, Delaney AJ and Sah P (2005) SK channels regulate excitatory synaptic transmission and plasticity in the lateral amygdala. *Nat Neurosci* **8**(5): 635-641.

Gan G, Yi H, Chen M, Sun L, Li W, Wu Y and Ding J (2008) Structural basis for toxin resistance of beta4-associated calcium-activated potassium (BK) channels. *J Biol Chem* **283**(35): 24177-24184.

Gross A and MacKinnon R (1996) Agitoxin footprinting the shaker potassium channel pore. *Neuron* **16**(2): 399-406.

Guex N and Peitsch MC (1997) SWISS-MODEL and the Swiss-PdbViewer: an environment for comparative protein modeling. *Electrophoresis* **18**(15): 2714-2723.

Hammond RS, Bond CT, Strassmaier T, Ngo-Anh TJ, Adelman JP, Maylie J and Stackman RW (2006) Small-conductance Ca^{2+}-activated K^+ channel type 2 (SK2) modulates hippocampal learning, memory, and synaptic plasticity. *J Neurosci* **26**(6): 1844-1853.

Han S, Yi H, Yin SJ, Chen ZY, Liu H, Cao ZJ, Wu YL and Li WX (2008) Structural basis of a potent peptide inhibitor designed for Kv1.3 channel, a therapeutic target of autoimmune disease. *J Biol Chem* **283**(27): 19058-19065.

Han S, Yin S, Yi H, Mouhat S, Qiu S, Cao Z, Sabatier JM, Wu Y and Li W (2010) Protein-protein recognition control by modulating electrostatic interactions. *J Proteome Res* **9**(6): 3118-3125.

Lange A, Giller K, Hornig S, Martin-Eauclaire MF, Pongs O, Becker S and Baldus M (2006) Toxin-induced conformational changes in a potassium channel revealed by solid-state NMR. *Nature* **440**(7086): 959-962.

Long SB, Campbell EB and Mackinnon R (2005) Crystal structure of a mammalian voltage-dependent Shaker family K^+ channel. *Science* **309**(5736): 897-903.

Lu Z, Klem AM and Ramu Y (2001) Ion conduction pore is conserved among potassium channels. *Nature* **413**(6858): 809-813.

MacKinnon R, Cohen SL, Kuo A, Lee A and Chait BT (1998) Structural conservation in prokaryotic and eukaryotic potassium channels. *Science* **280**(5360): 106-109.

Pease JH and Wemmer DE (1988) Solution structure of apamin determined by nuclear magnetic resonance and distance geometry. *Biochemistry* **27**(22): 8491-8498.

Regaya I, Beeton C, Ferrat G, Andreotti N, Darbon H, De Waard M and Sabatier JM (2004) Evidence for domain-specific recognition of SK and Kv channels by MTX and HsTx1 scorpion toxins. *J Biol Chem* **279**(53): 55690-55696.

Rodriguez de la Vega RC, Merino E, Becerril B and Possani LD (2003) Novel interactions between K+ channels and scorpion toxins. *Trends Pharmacol Sci* **24**(5): 222-227.

Rodriguez de la Vega RC and Possani LD (2004) Current views on scorpion toxins specific for K^+-channels. *Toxicon* **43**(8): 865-875.

Sabatier JM, Zerrouk H, Darbon H, Mabrouk K, Benslimane A, Rochat H, Martin-Eauclaire MF and Van Rietschoten J (1993) P05, a new leiurotoxin I-like scorpion toxin: synthesis and structure-activity relationships of the α-amidated analogue, a ligand of Ca2+-activated K+ channels with increased activity. *Biochemistry* **32**(11): 2763-2770.

Shakkotai VG, Regaya I, Wulff H, Fajloun Z, Tomita H, Fathallah M, Cahalan MD, Gargus JJ, Sabatier JM and Chandy KG (2001) Design and characterization of a highly selective peptide inhibitor of the small conductance calcium-activated K+ channel, SkCa2. *J Biol Chem* **276**(46): 43145-43151.

Stackman RW, Hammond RS, Linardatos E, Gerlach A, Maylie J, Adelman JP and Tzounopoulos T (2002) Small conductance Ca^{2+}-activated K^+ channels modulate synaptic plasticity and memory encoding. *J Neurosci* **22**(23): 10163-10171.

Stocker M (2004) Ca^{2+}-activated K^+ channels: molecular determinants and function of the SK family. *Nat Rev Neurosci* **5**(10): 758-770.

Subbotina J, Yarov-Yarovoy V, Lees-Miller J, Durdagi S, Guo J, Duff HJ and Noskov SY (2010) Structural refinement of the hERG1 pore and voltage-sensing domains with ROSETTA-membrane and molecular dynamics simulations. *Proteins* **78**(14): 2922-2934.

Tao X, Avalos JL, Chen J and MacKinnon R (2009) Crystal structure of the eukaryotic strong inward-rectifier K^+ channel Kir2.2 at 3.1 Å resolution. *Science* **326**(5960): 1668-1674.

Tseng GN, Sonawane KD, Korolkova YV, Zhang M, Liu J, Grishin EV and Guy HR (2007) Probing the outer mouth structure of the HERG channel with peptide toxin footprinting and molecular modeling. *Biophys J* **92**(10): 3524-3540.

Wang J, Cieplak, P., Kollman, P (1999) How Well Does a Restrained Electrostatic. *J Comput Chem* **21**: 1049-1074.

Wittekindt OH, Visan V, Tomita H, Imtiaz F, Gargus JJ, Lehmann-Horn F, Grissmer S and Morris-Rosendahl DJ (2004) An apamin- and scyllatoxin-insensitive isoform of the human SK3 channel. *Mol Pharmacol* **65**(3): 788-791.

Wu JJ, He LL, Zhou Z and Chi CW (2002) Gene expression, mutation, and structure-function relationship of scorpion toxin BmP05 active on SK_{Ca} channels. *Biochemistry* **41**(8): 2844-2849.

Wulff H and Zhorov BS (2008) K^+ channel modulators for the treatment of neurological disorders and autoimmune diseases. *Chem Rev* **108**(5): 1744-1773.

Yi H, Cao Z, Yin S, Dai C, Wu Y and Li W (2007) Interaction simulation of hERG K^+ channel with its specific BeKm-1 peptide: insights into the selectivity of molecular recognition. *J Proteome Res* **6**(2): 611-620.

Yin SJ, Jiang L, Yi H, Han S, Yang DW, Liu ML, Liu H, Cao ZJ, Wu YL and Li WX (2008) Different residues in channel turret determining the selectivity of ADWX-1 inhibitor peptide between Kv1.1 and Kv1.3 channels. *J Proteome Res* **7**(11): 4890-4897.

Yu L, Sun C, Song D, Shen J, Xu N, Gunasekera A, Hajduk PJ and Olejniczak ET (2005) Nuclear magnetic resonance structural studies of a potassium channel-charybdotoxin complex. *Biochemistry* **44**(48): 15834-15841.

FOOTNOTES

This work was supported by grants from the National Basic Research Program of China [Grant NO. 2010CB529800]; National High Technology Research and Development Program of China [Grant NO. 2012AA020304]; National Natural Sciences Foundation of China [Grants Nos. 30530140, 30973636, 31170789], New Century Excellent Talents in Wuhan University by Ministry of Education of China [Grant No. NCET-10-0651]; and Hubei Province Natural Sciences Foundation of China [Grant No. 2009CDA076].

FIGURE LEGENDS

Fig. 1. Selective recognition of SK3 channel by toxins with different channel-interacting surfaces. (a-c) Inhibition of SK3 channel currents by 100 nM ChTX, ADWX-1 or BmP05. BmP05 at 100 nM blocks approximately 80% of SK3 currents (c), whereas ChTX and ADWX-1 are almost inactive (a, b). (d) Dose-dependence of BmP05 block of SK3 currents. Fit of the curve provides an IC_{50} value of 3.76 ± 1.24 nM. (e-h) Different channel-interacting surfaces: ChTX (PDB code: 2CRD), ADWX-1 (PDB code: 2K4U), BmP05, and ScyTx (PDB code: 1SCY). All toxin basic residues are labeled in their channel binding surfaces.

Fig. 2. Decreased BmP05 potency for SK3 channel resulting from an increased content in basic residues in the BmP05 binding surface. (a) One or two arginine residue(s) (in red) was (were) introduced at the channel-interacting surface. (b-e) Representative current traces of the SK3 channel showing reduced inhibition by 100 nM BmP05 mutants. (b) 20.5% block by BmP05-S14R. (c) 30.5% block by BmP05-L15R. (d) 8.5% block by BmP05-N4R/S14R. (e) 10.7% block by BmP05-N4R/L15R. *$p < 0.05$ vs. control.

Fig. 3. Effects of substituting R^{485} and R^{489} by other basic residues on the SK3 blocking potency of BmP05. (a-h) Representative current traces of SK3 channel mutants showing current blocks by BmP05 and ChTX. (a-b) Absence of inhibition of SK3-R485H and SK3-R489H currents by 100 nM ChTX. (c-d) Significant inhibition of SK3-R485H and SK3-R489H currents by 100 nM BmP05. (e-f) Lack of inhibition of SK3-R485K and SK3-R489K channels by 100 nM ChTX. (g-h) Significant inhibition of SK3-R485K and SK3-R489K channels by 100 nM BmP05. (i) Concentration-dependence of SK3-R485H and SK3-R489H current blocks by BmP05. The data were fitted and yield IC_{50} values of 332.2 ± 84.9 nM (SK3-R485H) and 382.2 ± 141.1 nM (SK3-R489H). (j) Concentration-dependence of SK3-R485K and SK3-R489K current blocks by 100 nM BmP05. After fit, IC_{50} values are 145.0 ± 55.1 nM (SK3-R485K) and 191.8 ± 60.5 nM (SK3-R489K). Data represent the mean ± S.E. of at least three experiments, *$p < 0.05$.

Fig. 4. Effects of substituting R^{485} and R^{489} by acidic or polar residues on the SK3 blocking potency of BmP05. (a-h) Representative current traces of SK3 mutants showing current blocks by BmP05 and ChTX. (a-b) Reduced

inhibition of SK3-R485E and SK3-R489E channels by 100 nM BmP05. (c-d) Significant inhibition of SK3-R485E and SK3-R489E currents by 100 nM ChTX. (e-f) Reduced inhibition of SK3-R485S and SK3-R489S channels by 100 nM BmP05. (g-h) Significant inhibition of SK3-R485S and SK3-R489S currents by 100 nM ChTX. (i) Concentration-dependence of SK3-R485E and SK3-R489E current blocks by ChTX. Fits of the data yield IC_{50} values of 381.7 ± 84.1 nM (SK3-R485E) and 110.7 ± 28.1 nM (SK3-R489E). (j) Concentration-dependence of SK3-R485S and SK3-R489S current blocks by 100 nM ChTX. Fits yield IC_{50} values of 84.8 ± 21.6 nM (SK3-R485S) and 30.2 ± 4.5 nM (SK3-R489S). Data represent the mean ± S.E. of at least three experiments, $*p < 0.05$.

Fig. 5. Importance of other amino acid residues of the SK3 channel outer vestibule on the potency of BmP05 and ChTX. (a-j) Representative current traces of SK3 channel mutants showing current blocks by BmP05 and ChTX. (a, d) Reduced inhibition of SK3-D492N and SK3-D518N currents by 100 nM BmP05. (b, c and e) Significant inhibition of SK3-Q493A, SK3-D495N, and SK3-H522A currents by 100 nM BmP05. (f-j) Decreased inhibition of SK3-D492N, SK3-Q493A, SK3-D495N, SK3-D518N, and SK3-H522A currents by 100 nM ChTX. (k) Average inhibition of wild-type and mutant SK3 channel currents by 100 nM BmP05. (l) Average inhibition of wild-type and mutant SK3 channel currents by 100 nM ChTX. $*p < 0.05$ vs. control.

Fig. 6. Mechanism of selective SK3 channel recognition by scorpion toxins, as addressed by molecular modeling and docking simulation approaches. (a) Top view of the narrow gateway in the SK3 channel turrets. The large and small rings of basic residues are designated by dashed lines, colored yellow and purple, respectively. (b). Molecular surface representation of the SK3 channel vestibule. Basic residues are in blue and acidic residues are in red, as viewed from the extracellular side. (c) Interaction details of BmP05-SK3 complex viewed from the extracellular side. To better distinguish between BmP05 and SK3 channel, the toxin is colored in green and SK3 channel in grey. (d) K^6 residue of BmP05 plugged into SK3 channel pore. The A and C chains were colored in yellow and in cyan, respectively. (e-f) The functional residues within one SK3 channel turret that associate with R^7 and R^{13} residues of BmP05 within a distance of 4 Å. The B and C chains were colored in green and in cyan, respectively.

Figure 1

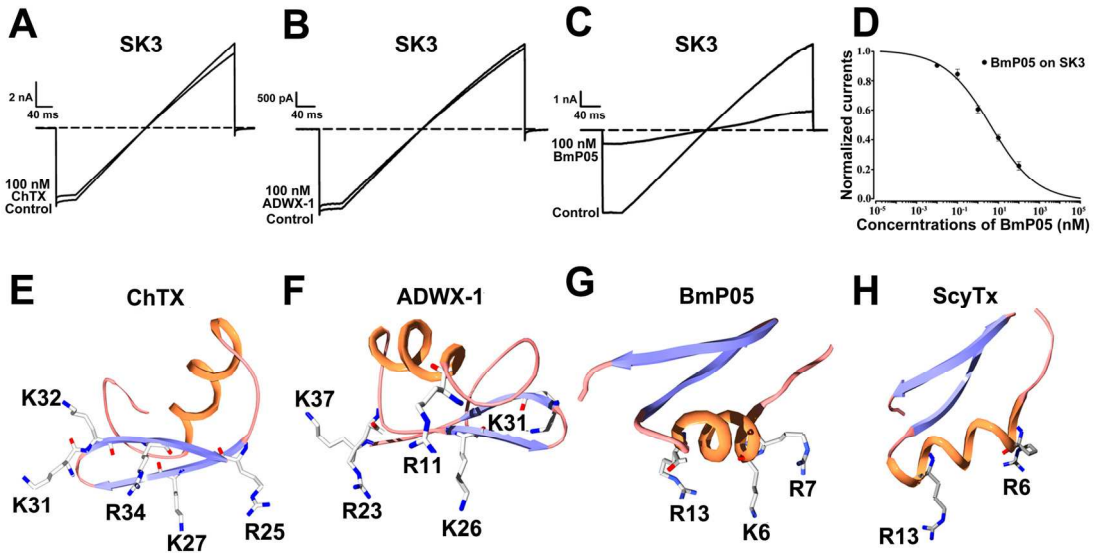


Figure 2

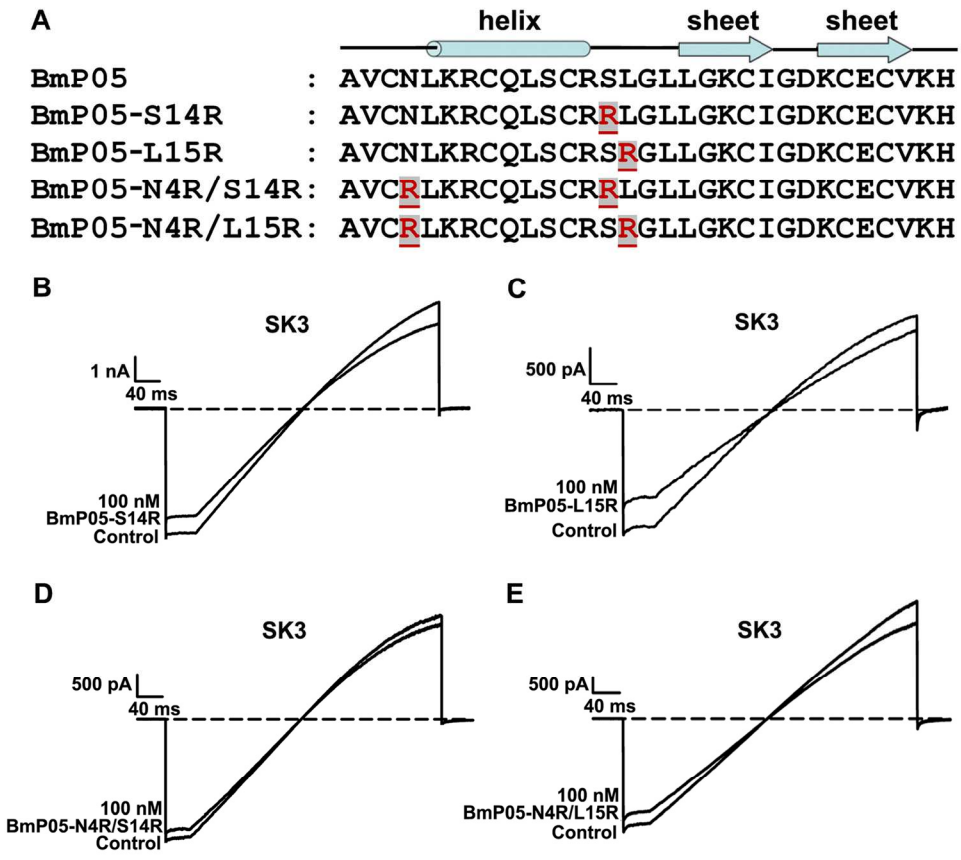


Figure 3

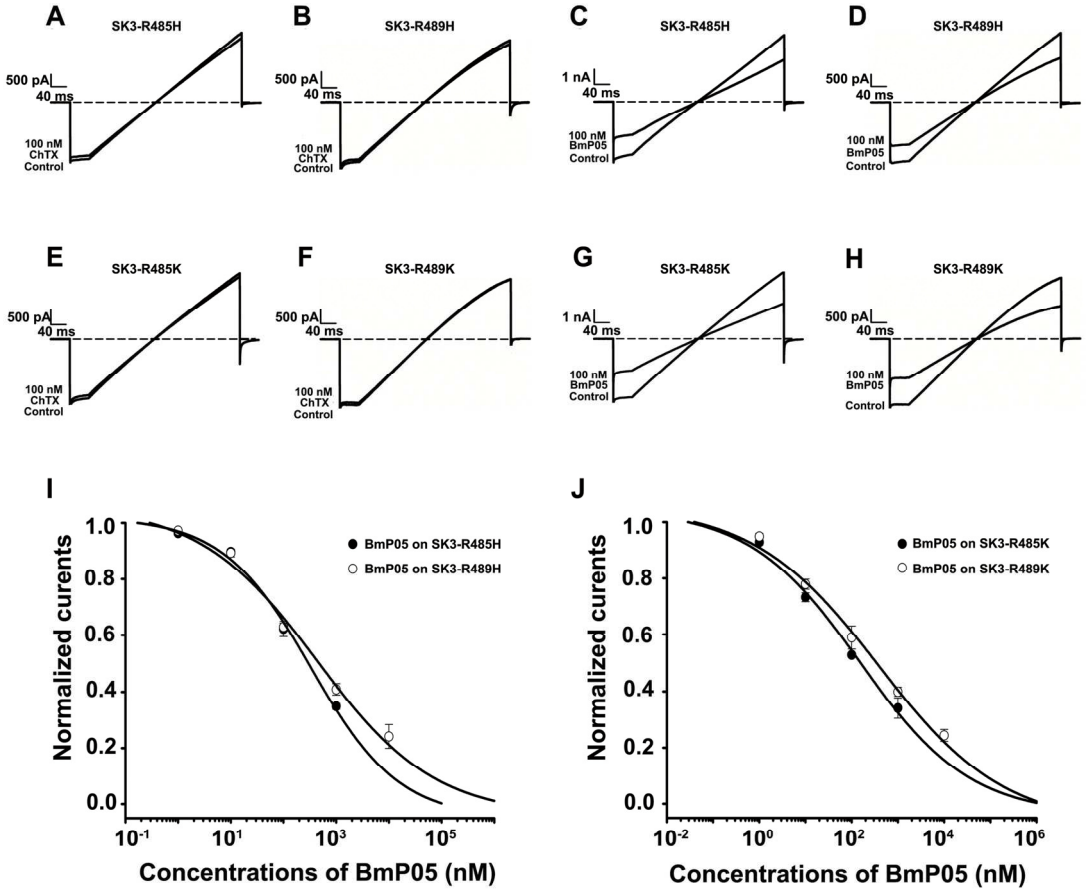

A
SK3-R485H
500 pA
40 ms
100 nM ChTX Control
B
SK3-R489H
500 pA
40 ms
100 nM ChTX Control
C
SK3-R485H
1 nA
40 ms
100 nM BmP05 Control
D
SK3-R489H
500 pA
40 ms
100 nM BmP05 Control
E
SK3-R485K
500 pA
40 ms
100 nM ChTX Control
F
SK3-R489K
500 pA
40 ms
100 nM ChTX Control
G
SK3-R485K
1 nA
40 ms
100 nM BmP05 Control
H
SK3-R489K
500 pA
40 ms
100 nM BmP05 Control
I
Normalized curents
BmP05 on SK3-R485H
BmP05 on SK3-R489H
Concentrations of BmP05 (nM)
J
Normalized curents
BmP05 on SK3-R485K
BmP05 on SK3-R489K
Concentrations of BmP05 (nM)

Figure 4

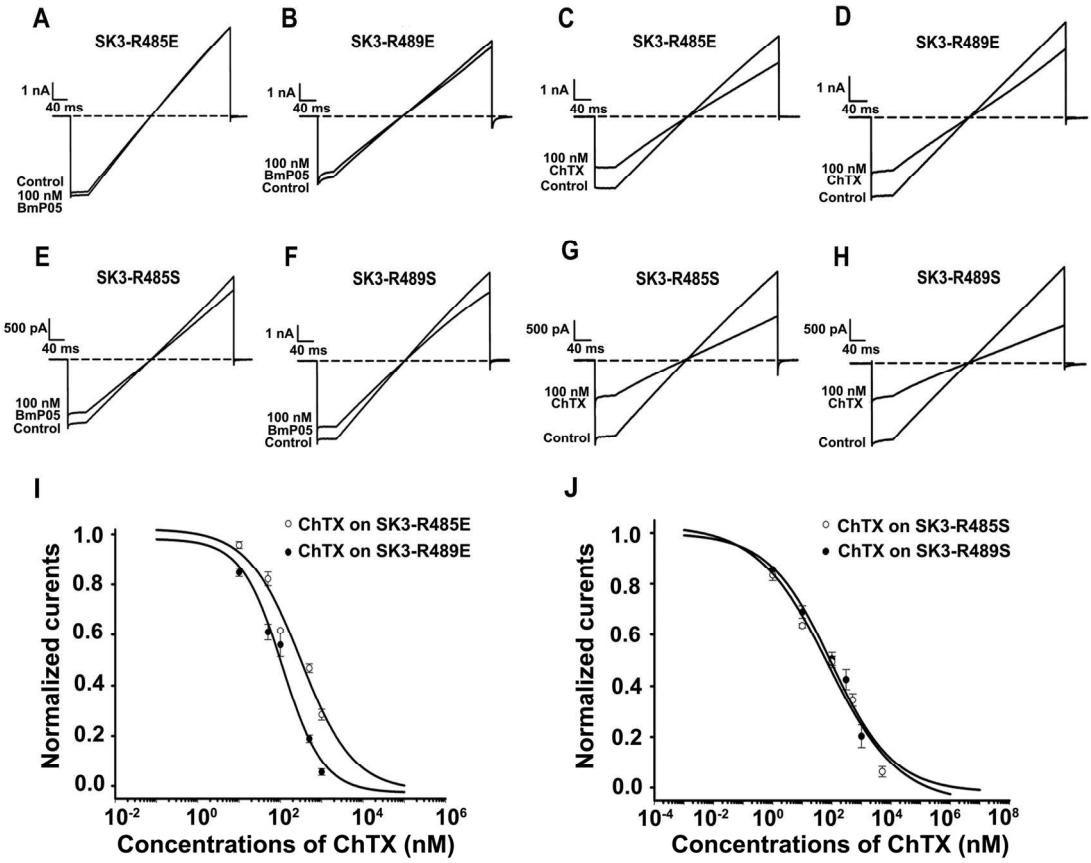

A
SK3-R485E
1 nA
40 ms
Control
100 nM
BmP05
B
SK3-R489E
1 nA
40 ms
100 nM
BmP05
Control
C
SK3-R485E
1 nA
40 ms
100 nM
ChTX
Control
D
SK3-R489E
1 nA
40 ms
100 nM
ChTX
Control
E
SK3-R485S
500 pA
40 ms
100 nM
BmP05
Control
F
SK3-R489S
1 nA
40 ms
100 nM
BmP05
Control
G
SK3-R485S
500 pA
40 ms
100 nM
ChTX
Control
H
SK3-R489S
500 pA
40 ms
100 nM
ChTX
Control
I
ChTX on SK3-R485E
ChTX on SK3-R489E
Normalized curents
1.0
0.8
0.6
0.4
0.2
0.0
10-2
100
102
104
106
Concentrations of ChTX (nM)
J
ChTX on SK3-R485S
ChTX on SK3-R489S
Normalized curents
1.0
0.8
0.6
0.4
0.2
0.0
10-4
10-2
100
102
104
106
108
Concentrations of ChTX (nM)

Figure 5

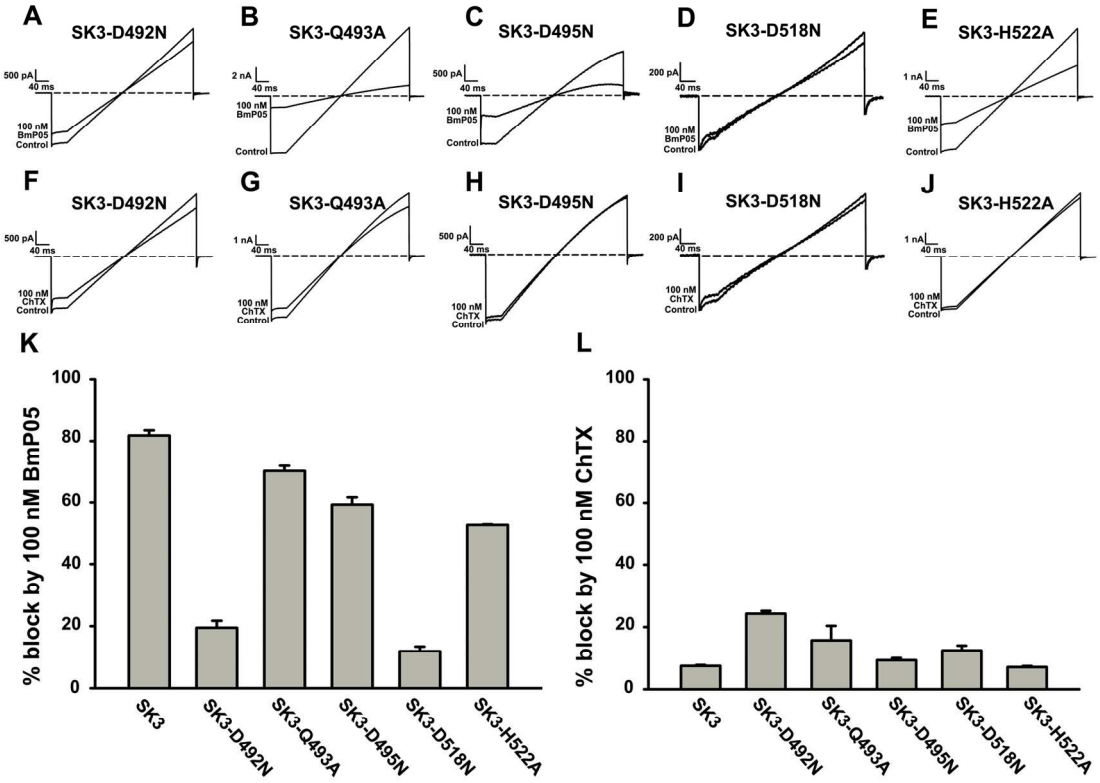
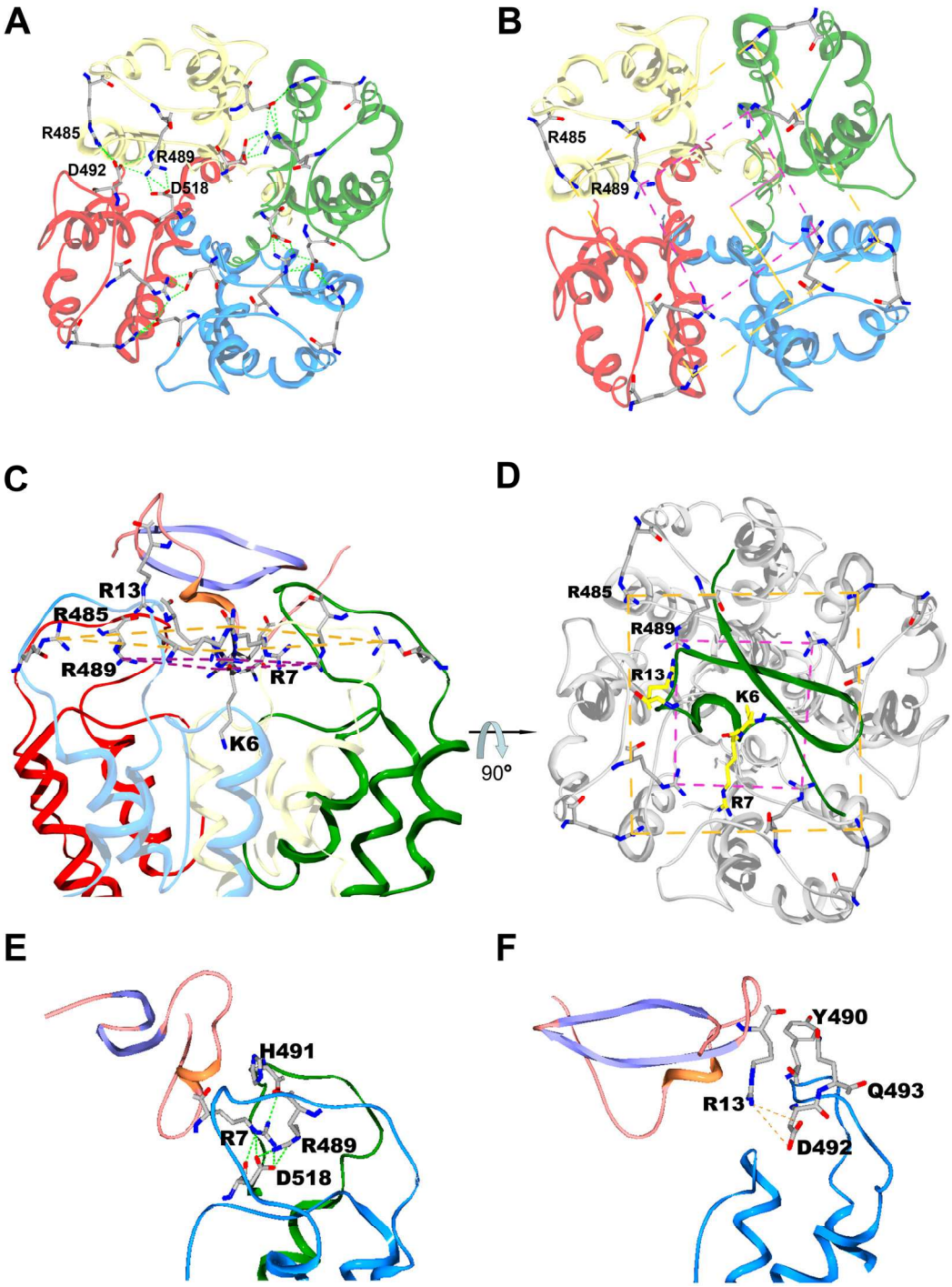

A
SK3-D492N
500 pA
40 ms
100 nM BmP05
Control
B
SK3-Q493A
2 nA
40 ms
100 nM BmP05
Control
C
SK3-D495N
500 pA
40 ms
100 nM BmP05
Control
D
SK3-D518N
200 pA
40 ms
100 nM BmP05
Control
E
SK3-H522A
1 nA
40 ms
100 nM BmP05
Control
F
SK3-D492N
500 pA
40 ms
100 nM ChTX
Control
G
SK3-Q493A
1 nA
40 ms
100 nM ChTX
Control
H
SK3-D495N
500 pA
40 ms
100 nM ChTX
Control
I
SK3-D518N
200 pA
40 ms
100 nM ChTX
Control
J
SK3-H522A
1 nA
40 ms
100 nM ChTX
Control
K
% block by 100 nM BmP05
100
80
60
40
20
0
SK3
SK3-D492N
SK3-Q493A
SK3-D495N
SK3-D518N
SK3-H522A
L
% block by 100 nM ChTX
100
80
60
40
20
0
SK3
SK3-D492N
SK3-Q493A
SK3-D495N
SK3-D518N
SK3-H522A

Figure 6


A
R485
R489
D492
D518
B
R485
R489
C
R13
R485
R489
R7
K6
90°
D
R485
R489
R13
K6
R7
E
H491
R7
R489
D518
F
Y490
Q493
R13
D492